A Model for Prediction of Auditory Tissue Damage in Fish

Final Report

Submitted to the:

Joint Industry Program (JIP) on E&P Sound and Marine Life

By

Dr. Mardi C. Hastings
The Pennsylvania State University
Applied Research Laboratory
State College, PA 16804

May 23, 2009

INTRODUCTION

Objective

The purpose of this study is to show that a mathematical model of the biomechanics of the peripheral auditory system in fishes (Danak and Hastings, 2001; Finneran and Hastings, 2000) could be used to predict the onset of auditory tissue damage in different species and sizes. The model calculates relative motion between the sensory epithelia and overlying otolith in the inner ear. Excessive relative motion at this interface is believed to cause loss of the apical ciliary bundles of hair cells embedded in the epithelium.

Hypotheses Tested

Biological systems exhibit different forms of biomechanical failure, which result in tissue damage or injury. The primary hypothesis tested in this study is that acoustic trauma results when the inner ear receives excessive stimulation, which can then be correlated with different types and degrees of damage. A secondary hypothesis tested is that acoustic trauma in the inner ear will correlate with one or more sound exposure metrics (i.e., peak sound pressure level, sound exposure level, rise time, kurtosis, etc.). If a correlation is found this would link observed auditory tissue damage with metrics that can be determined *a priori* for different types of field operations.

Summary of Methods and Approach

A biomechanical mathematical model based on fish anatomy and morphology was revised to calculate the relative motion between the sensory epithelium and saccular otolith in the inner ear for defined sound exposures as reported in the literature for three previous studies: Hastings et al. 1996; McCauley et al. 2003; and Popper et al. 2005. Each of these studies reported hair cell damage or hearing loss following sound exposure. These results along with applicable sound exposure metrics from each study were tabulated in a table to relate inner ear acoustic trauma and exposure metrics with observed damage.

Background

Several studies in the literature report existence or nonexistence of auditory tissue damage in fishes exposed to different types of acoustic signals — i.e., continuous tones, low frequency sonar emissions, and air-gun shots. The relationship between signal characteristics and observed damage, however, is not understood. In fact little has been done to determine the relationship between sound exposures known to produce damage and underlying mechanisms associated with interaction of a sound wave with the body of a fish and its inner ear. Although acoustic waveforms have different characteristics, mechanical failure in healthy tissue generally occurs when its dynamic stress-strain state exceeds a limit beyond which membranes at the cellular or organ level rupture or tear. The biomechanical mathematical model used in this study provides a common basis to relate similar types of damage to different types of acoustic exposures. Because it is based on basic principles of fluid, bio, and solid mechanics, parameters can be changed to predict occurrence of auditory tissue damage in different species of fish for predefined acoustic signals.

METHODS

Finneran and Hastings (2000) and Danak and Hastings (2001) developed mathematical models for the peripheral auditory systems in goldfish and American shad, respectively, to investigate their steady-state frequency response to sound. Because the acoustic wavelengths for the frequency ranges of interest are much larger than the anatomical structures in the auditory periphery, they analyzed each part of the anatomy using lumped-parameter elements. Mechanical and fluid system elements were used to represent the swim bladder, Weberian apparatus and saccule in goldfish, and the swim bladder, precoelomic duct connecting swim bladder and auditory bullae, utricle, and saccule in American shad. Equations of motion were written for each piece of the system. Values needed for surface areas, masses, inertias, damping constants, spring constants, fluid resistances, fluid compliances, and acoustic impedances were either measured, found in the literature, or indirectly determined from swim bladder resonance data. Details regarding the equations and parameter values can be found in Finneran and Hastings (2000) and Danak and Hastings (2001).

The ultimate goal of these mechanical and fluid system models was to predict shearing of the ciliary bundles in the inner ear resulting from relative displacement between the sensory epithelium and overlying otolith in the inner ear. So a mechanical system model for the ciliary bundles was also developed and integrated in the system of equations for this purpose. The results of these studies showed good agreement between auditory sensitivity previously determined in behavioral studies and the model's predictions based on relative displacement in the inner ear.

Application to specific species

The existing models for the peripheral auditory systems of fishes were updated to run on MATLAB® Version 7.3.0 (R2006b). Two programs were developed, one for fish with Weberian ossicles and another for those without. The MATLAB® scripts for these programs, WOFish and GenFish, respectively, are listed in Appendix A. Next anatomical and hearing data were collected for the species tested by Hastings et al. (1996), McCauley et al. (2003), and Popper et al. (2005). These species are the oscar (*Astronotus ocellatus*), pink snapper (*Pagrus auratus*), lake chub (*Couesius plumbeus*), northern pike (*Esox lucius*), and broad whitefish (*Coregonus nasus*). Of these five, only the lake chub has Weberian ossicles.

Mann et al. (2007) reported auditory evoked potential threshold data for the lake chub, northern pike and broad whitefish used by Popper et al. (2005). Behavioral hearing thresholds for oscars of the same size used by Hastings et al. (1996) were previously published by Yan and Popper (1992), and AEP thresholds of similarly sized specimens were published by Kenyon et al. (1998). No hearing data were found for pink snapper; however, a behavioral audiogram for a fish of the same genus, the red seabream (*Pagrus major*) – also found in Pacific waters – was published by Ishioka et al. (1988). These data were used for correlation with the biomechanical model for the pink snapper. Figure 1 displays a summary of these audiograms.

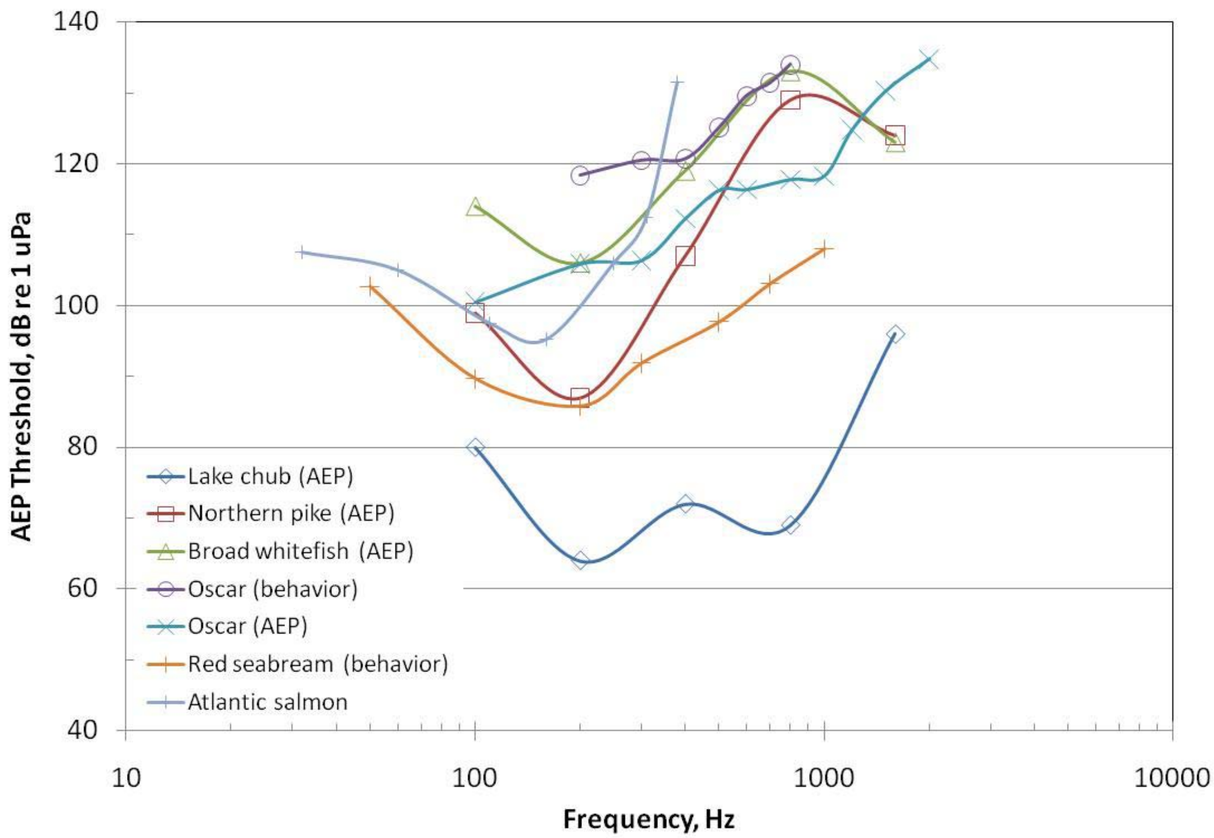

Figure 1: Audiograms for species considered in this study: Lake chub, northern pike, and broad whitefish AEP data from Mann et al. (2007); oscar behavioral data from Yan and Popper (1992); oscar AEP data from Kenyon et al. (1998); and red seabream (*Pagrus major*) data (a proxy for the pink snapper, *Pagrus auratus*) from Ishioka et al. (1988). The lake chub has Weberian ossicles connecting the anterior swim bladder to the inner ear (saccule) so it has lower thresholds than the others. The behavioral auditory thresholds of Atlantic salmon (*Salmo salar*) from Hawkins and Johnstone (1978) are shown for comparison. The only other salmonid in this group is the broad whitefish.

Geometrical and anatomical data are also needed for the biomechanical model. These data were found in the literature or estimated by scaling available information. Mann et al. (2007) provided overall lengths and masses, and Song et al. (2008) provided detailed information about the inner ear for the species used by Popper et al. (2005). A summary of mass-length data and an X-ray of an oscar provided by Derenburger (1997) were used to determine geometrical parameters needed for its model. Little information was available for the pink snapper. McCauley et al. (2003) reported only average lengths. Mass was estimated using mass-length data from Ishioka et al. (1988) for red seabream, swim bladder dimensions were scaled from image data for rainbow trout (*Oncorhynchus mykiss*) found in Popper et al. (2007), and inner ear geometry was scaled from image data for northern pike in Song et al. (2008). Table 1 provides a summary of the species considered and geometrical parameters used for their models.

Table 1. Physical parameters of experimental fishes

Species	Std. Length (mm)	Mass (g)	Otolith length (mm)	Otolith diameter (mm)	Swim bladder radius (mm)	References
Lake chub (*Couesius plumbeus*)	88	8.6	1.57	0.29	6.14**	Popper et al. (2005) Mann et al. (2007) Song et al. (2008)
Northern pike (*Esox lucius*)	490	1147	6.55	1.72	21.6^^	Popper et al. (2005) Mann et al. (2007) Song et al. (2008)
Broad whitefish (*Coregonus nasus*)	408	1367	5.45*	1.43*	18.0^^	Popper et al. (2005) Mann et al. (2007) Song et al. (2008)
Pink snapper (*Pagrus auratus*)	230	343^	3.07*	0.81*	10.1^^	McCauley et al. (2003)
Oscar (*Astronotus ocellatus*)	83	26.4	2.78	1.11	5.99	Derenburger (1997) Hastings et al. (1996)
	* Scaled with length from Northern Pike values ^ Scaled from length-mass data for *Pagrus major* (Ishioka et al. 1988) ** Scaled with length from goldfish values (Finneran and Hastings 2000) ^^ Scaled with length from image data for *Oncorhynchus mykiss* (Popper et al. 2007)					

RESULTS

Auditory Sensitivity

Figures 2 – 6 show the correlation between auditory sensitivity predicted by the model and auditory sensitivities calculated from the audiogram data of Figure 1. Auditory sensitivity from the model is the amplitude of relative displacement between the sensory epithelium and otolith in the saccule per 1 Pa of acoustic pressure. This relative displacement provides the adequate stimulus to bend the apical ciliary bundles of the hair cells, which activates them to send action potentials to the brain. The relative displacement (nm/Pa) from the model is correlated with auditory thresholds by taking their reciprocals, normalizing them at or near the point of highest sensitivity (i.e., lowest threshold), and then visually curve fitting the relative displacement by adjusting unknown (but bounded) stiffness and damping parameters in the model. Stiffness and damping parameters for the swim bladder and Weberian ossicles can also be obtained from dynamic testing of individual fish specimens as was done by Finneran and Hastings (2000) for goldfish. Results presented in the following figures indicate that the geometry and anatomy of the peripheral auditory system play major roles in defining the shape of the audiogram in fishes.

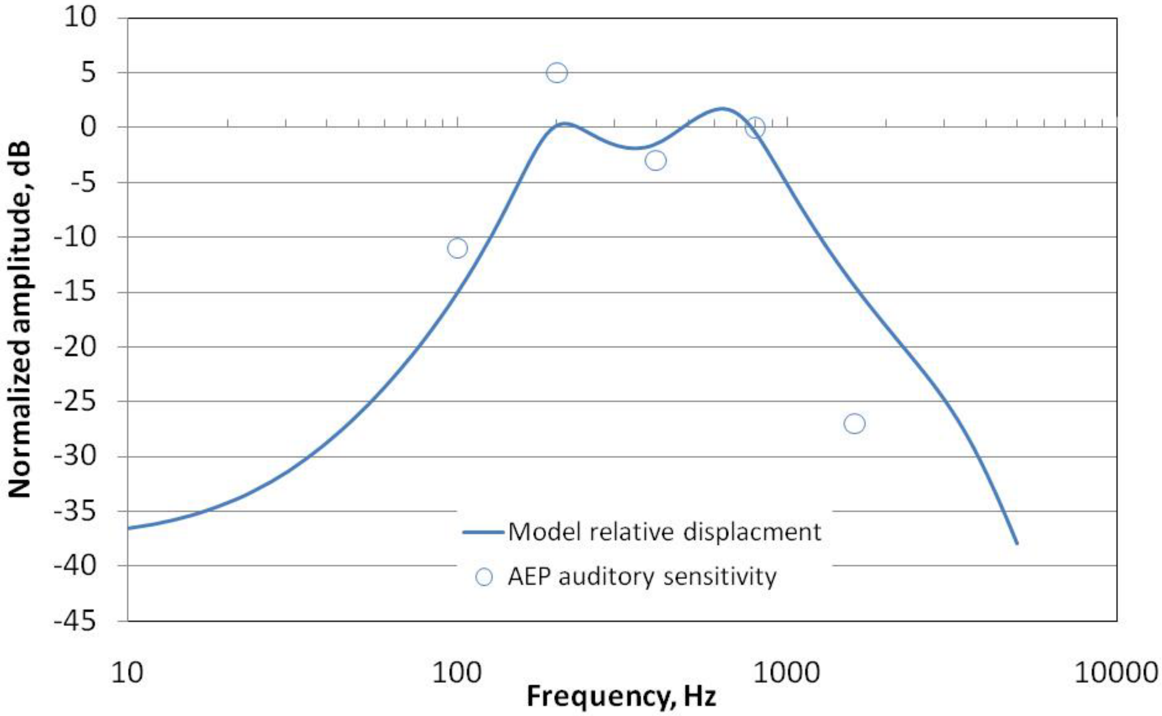

Figure 2: Results of model for **lake chub** (*Couesius plumbeus*) showing good agreement with auditory sensitivity determined from AEP hearing thresholds measured by Mann et al. (2007).

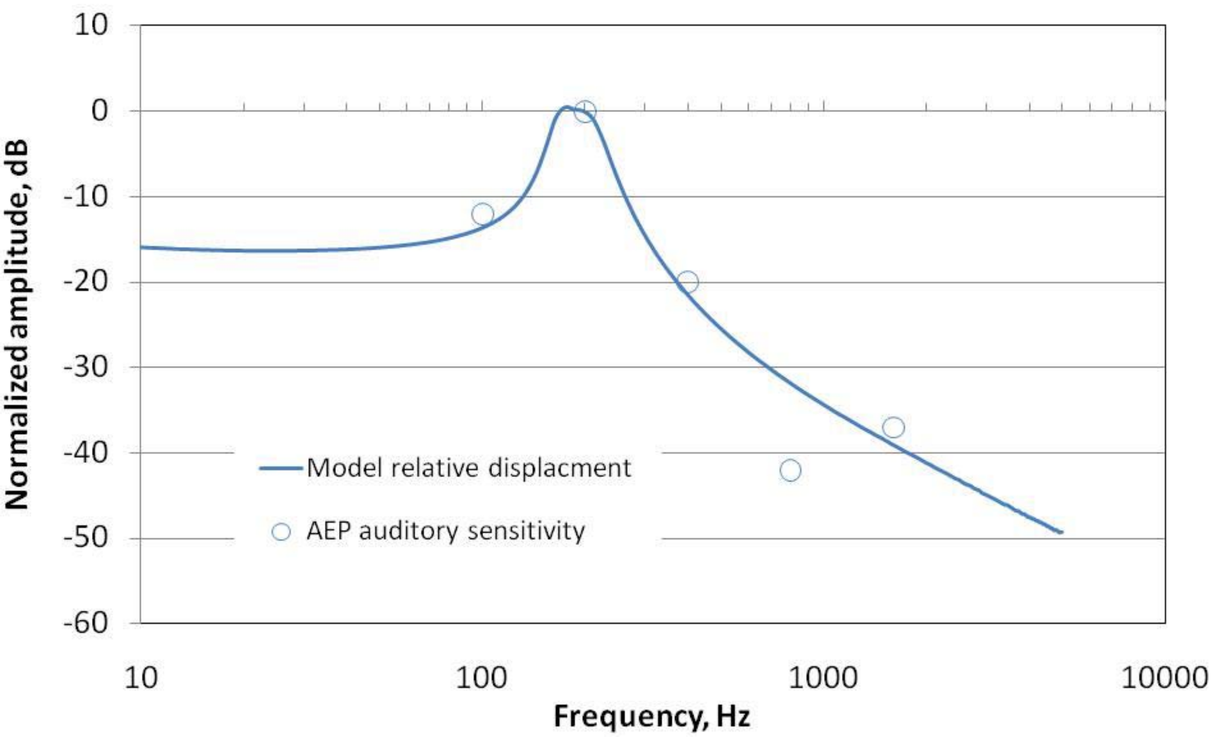

Figure 3: Results of model for **northern pike** (*Esox lucius*) showing good agreement with auditory sensitivity determined from AEP hearing thresholds measured by Mann et al. (2007).

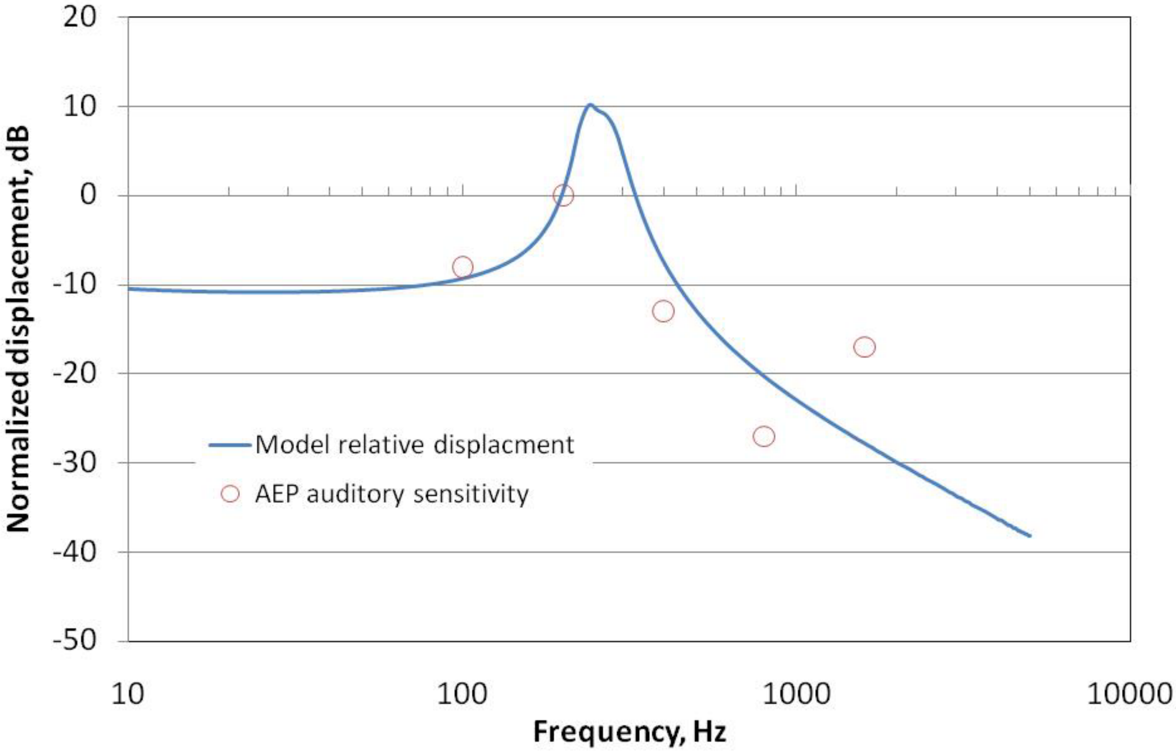

Figure 4: Results of model for **broad whitefish** (*Coregonus nasus*) showing good agreement with auditory sensitivity determined from AEP hearing thresholds measured by Mann et al. (2007).

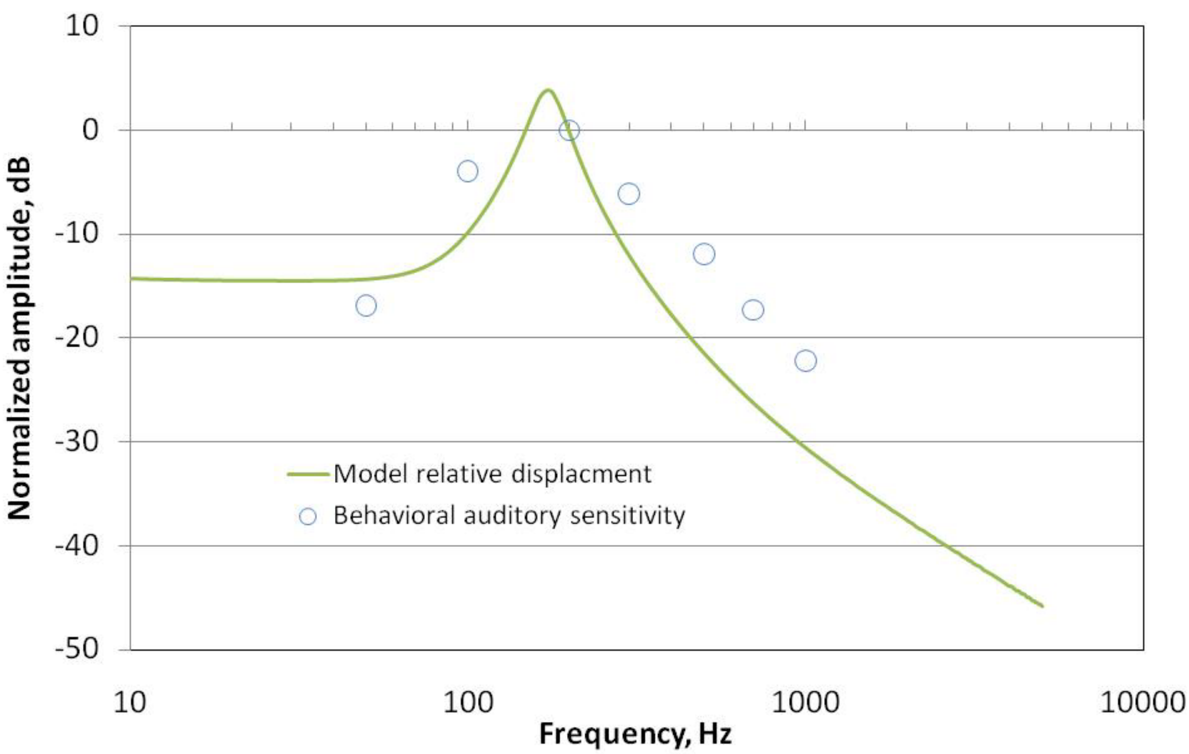

Figure 5: Results of model for **pink snapper** (*Pagrus auratus)* showing good agreement with auditory sensitivity estimated from behavioral thresholds for *Pagrus major* (Ishioka et al. 1988).

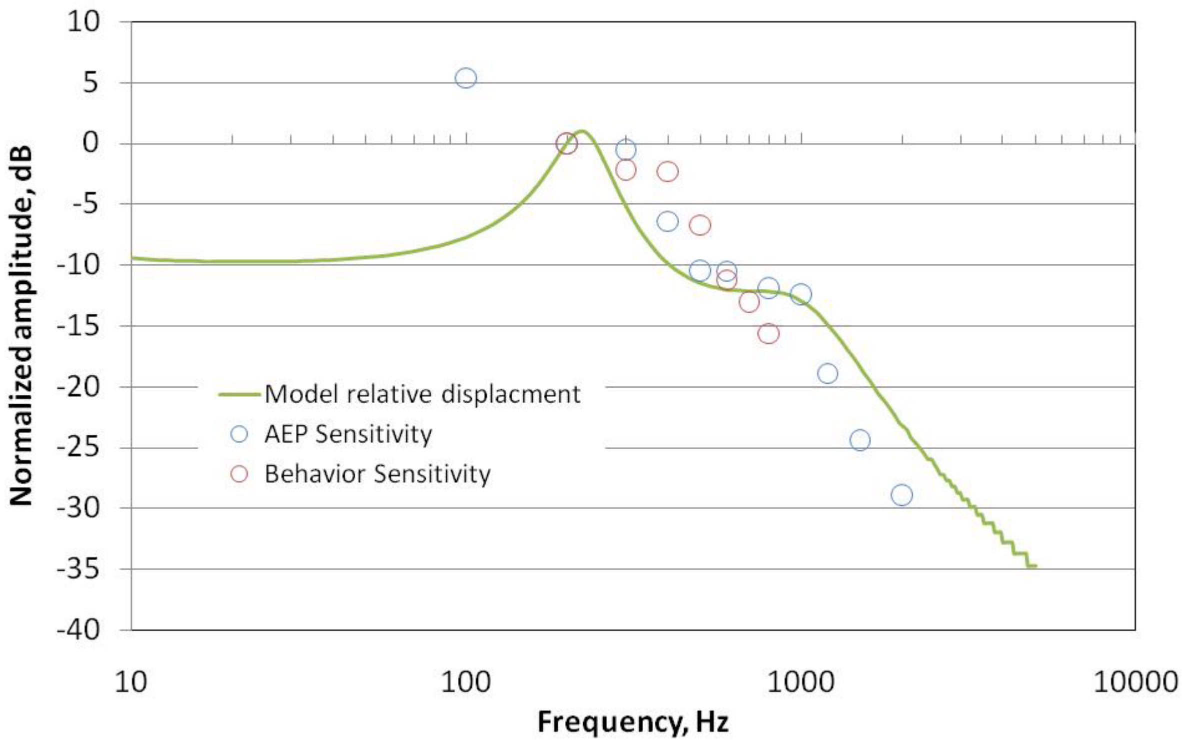

Figure 6: Results of model for the **oscar** (*Astronotus ocellatus*) showing good agreement with auditory sensitivity estimated from AEP (Kenyon et al. 1998) and behavioral (Yan and Popper 1992) thresholds. [Note that auditory threshold measurements below 200 Hz may be affected by perception with the lateral line and oftentimes indicate unusually high sensitivity.]

The output of the model is relative displacement per unit acoustic pressure in nm/Pa. Thus the relative displacement due to an impinging sound can be calculated by multiplying the model output and the acoustic pressure acting on the fish (i.e., the input). The relative displacement at threshold can also be estimated by multiplying the output of the model and the acoustic pressure corresponding to the auditory threshold. Excessive relative motion can be evaluated by comparing these two relative displacement amplitudes.

Prediction of Excessive Relative Motion in the Inner Ear from Sound

The effects of three signals on relative displacements in the inner ears of these fishes were investigated. The first signal was a pure tone at 300 Hz with a peak SPL of 180 dB re 1 μPa that was found to cause a very small amount of hair cell damage in the oscar after a 60-minute exposure (Hastings et al. 1996). The second one was a received signal from an airgun array as reported by Popper et al. (2005). Lake chub and northern pike exposed to multiple shots of this signal had temporary threshold shift (TTS), but no hair cell damage. The third signal was from a single airgun recorded at the fish cage from two different ranges as reported by McCauley et al. (2003). One group of pink snappers exposed to this signal for approximately 1 ½ hours over a 3 hour period were reported to have hair cell damage in the saccule that increased while they were held 58-days post exposure.

The two airgun signals were graphically broken down in frequency bands. An average sound pressure level for each band was calculated and used to multiply the output of the model for each species. Appendix B provides a tabular summary of the bands for each signal. This process accounts for the change in sensitivity of the fish's ear with frequency in addition to the frequency content of the signal. Figures 7 – 11 present the results of this analysis. Each figure shows the relative motion (nm) in the inner ear in response to each of these signals contrasted with the relative motion in the inner ear at pressure levels reported for thresholds (open circles).

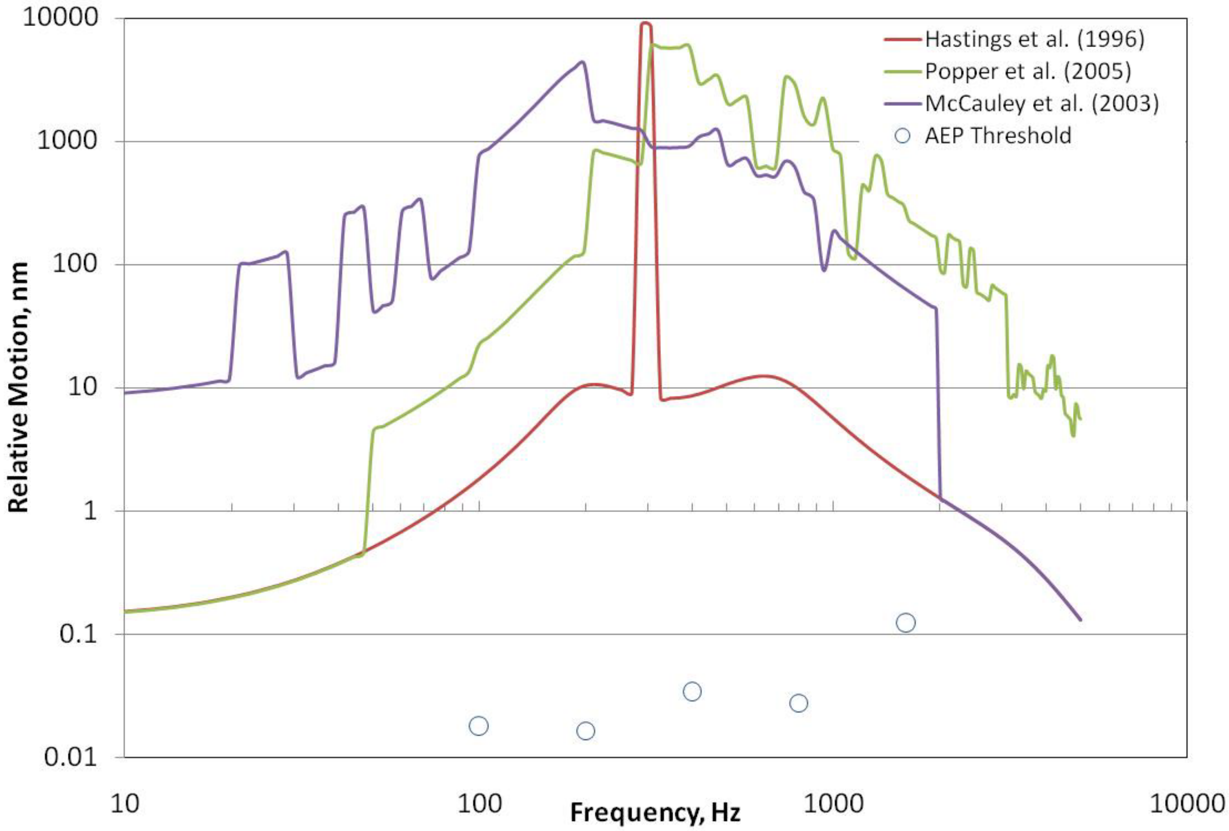

Figure 7: Results of exposure analysis for **lake chub** (*Couesius plumbeus*). **Popper et al. (2005)** found TTS in lake chub at 200, 400, 800 and 1600 Hz, with the largest amount (~35 dB) at 400 Hz after 20 shots. Responses to signals from the other studies are shown for comparison.

The results for lake chub in Figure 7 clearly show the largest relative motion (green curve) at the frequency (400 Hz) where the maximum amount of TTS occurred. The relative motion at threshold level is over five orders of magnitude smaller than the largest relative motion at this frequency. Figures 8 and 9 summarize the results for the other two species tested by Popper et al. (2005). The largest relative motion for northern pike and broad whitefish also occurs around 400 Hz; however, its amplitude is about an order of magnitude smaller than the relative motion in the lake chub for the same stimulus. The signal spectrum level in this study did not have any energy below 50 Hz, and very little energy below 200 Hz. So the stimulus is most prominent at frequencies above 200 Hz. The broad whitefish (Figure 9) did not experience TTS. It is interesting to note that the ratio between the largest relative motion and the relative motion associated with the hearing threshold at 400 Hz is the smallest of these three species.

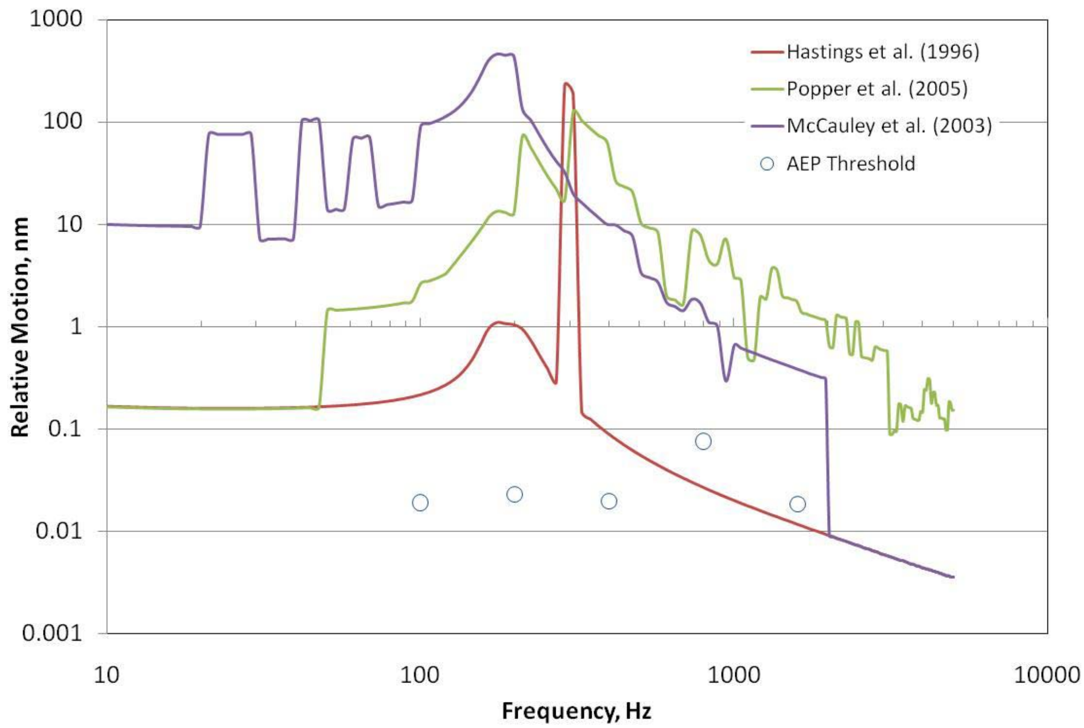

Figure 8: Results of exposure analysis for **northern pike** (*Esox lucius*). **Popper et al. (2005)** found TTS in northern pike at 100, 200, and 400 Hz, with the largest amount (~25 dB) at 400 Hz after 5 shots.

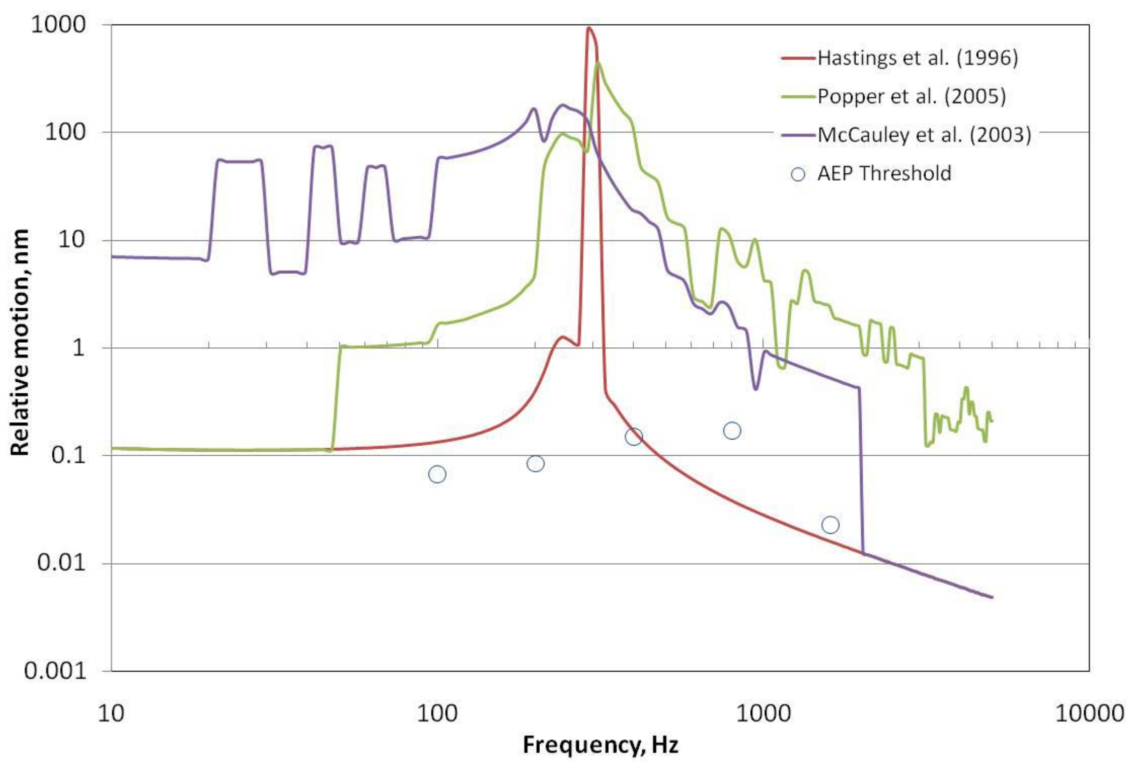

Figure 9: Results of exposure analysis for **broad whitefish** (*Coregonus nasus*), a salmonid. **Popper et al. (2005)** found no TTS in broad whitefish after 5 shots from the airgun array.

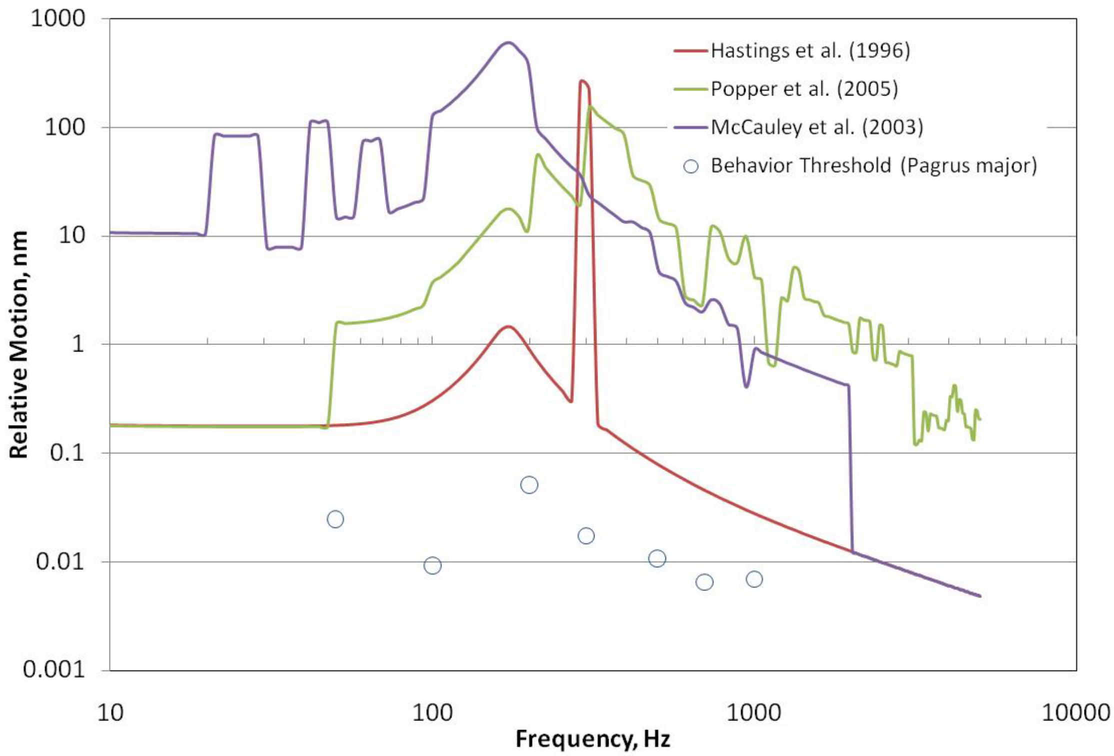

Figure 10: Results of exposure analysis for **pink snapper** (*Pagrus auratus*). **McCauley et al. (2003)** reported hair cell damage localized at the caudal end of the saccule in pink snapper held 58 days post-exposure. Note that the largest relative motion (purple line) occurs at frequencies less than 200 Hz.

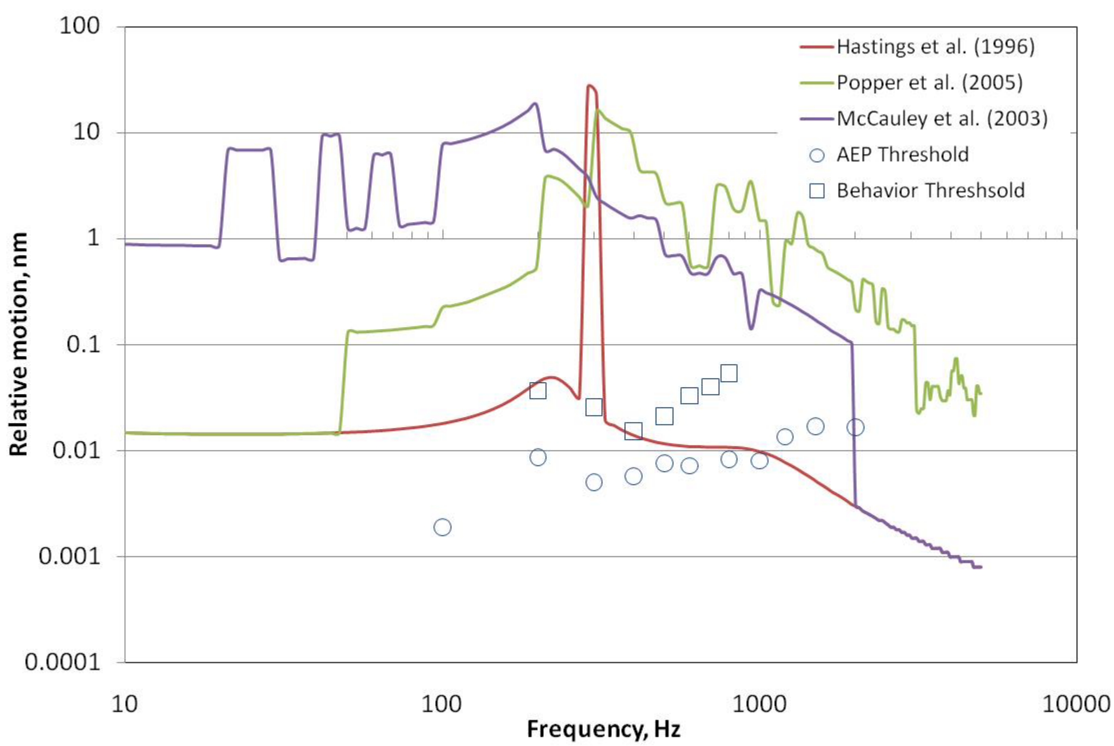

Figure 11: Results of exposure analysis for **oscars** (*Astronotus ocellatus*). **Hastings et al. (1996)** found some hair cell damage after 3 days following exposure to 180-dB, 300-Hz pure tone for 60 minutes.

In contrast to the sound exposures reported by Popper et al. (2005), the sound spectrum level in the McCauley et al. (2003) study contained the highest energy at frequencies below 200 Hz. In addition the pink snapper has relatively sensitive hearing at low frequencies; consequently, the ratio of maximum relative motion to the relative motion associated with threshold is at least four orders of magnitude as indicated in Figure 10. Enger (1981) found that hair cells were damaged in the caudal end of the saccule in cod (*Gadus morhua*) when exposed to intense tones at 50 Hz. Exposure to tones at higher frequencies caused damage to the mid and rostral portions of the saccular epithelium. This is consistent with McCauley et al. (2003) reporting hair cell damage localized in the caudal end of the saccule. Neither of these studies measured hearing thresholds so it is unknown if such localized damage has any effect on auditory thresholds, even at low frequencies.

Formulation of Metrics

Table 2 summarizes metrics common to all three studies considered here. SEL has been found to correlate with increasing TTS in aquatic mammals, but the SEL associated with onset of TTS varies among species. So it is not necessarily expected to be a predictor for the onset of TTS or auditory tissue damage in fishes. The results of this study suggest that the absolute maximum relative motion between the sensory epithelium and otolith in the inner ear, or even more so, the ratio of the maximum relative motion to the motion associated with hearing threshold at the same frequency – i.e., the "excess relative motion" expressed in dB – could be indicative of hearing loss and/or auditory tissue damage. The latter metric would account for the significance of the sound source frequency bands of maximum energy overlapping with the most sensitive auditory frequencies in any given species. Figures 7 – 11 show some amplification of the relative motion at the frequencies of most sensitive hearing for all the species and signals considered here.

Except for the oscar, the values of "excess relative motion" are consistent with the associated acoustic trauma. For the other four species, the broad whitefish with the smallest excess relative motion (67 dB) did not experience any hearing loss or tissue damage, and northern pike with 75.4 dB excess relative motion had TTS that recovered within 18 hours. Lake chub has the highest value (107 dB) and these animals experienced asymptotic TTS (i.e., so high that additional sound exposure will not cause higher levels of threshold shift). In addition one group of lake chub did not recover from TTS before the Popper et al. (2005) study ended, but no test subjects were held longer than 48 hours to see if hair cell damage developed over time. To date, McCauley et al. (2003) is the only reported exposure study that held specimens longer than 2-3 days to examine them for hair cell damage.

The excess relative motion for oscars is undervalued in Table 2 because they were tested in a waveguide with flexible walls, so the sound speed was actually much smaller than the speed of sound in open water that was used in the model. Therefore the model prediction for relative motion from the direct field is much smaller than that actually experienced by the specimens during testing. This experimental caveat was pointed out by Hastings et al. (1996).

Table 2. Summary of available metrics associated with sound exposure studies by Hastings et al. (1996), McCauley et al. (2003), and Popper et al. (2005)

	Lake chub (*Couesius plumbeus*)	Northern pike (*Esox lucius*)	Broad whitefish (*Coregonus nasus*)	Pink snapper (*Pagrus auratus*)	Oscar (*Astronotus ocellatus*)
Acoustic trauma	TTS	TTS	none	Hair cell (caudal saccule)	Hair cell (small amt. in striola of lagena and utricle)
Post-exposure time				58 days	3 days
Wild caught	yes	yes	yes	no	no
Length ratio to full adult*	0.38	0.34	0.57	0.20	0.18
Source type	Airgun array (12 L)	Airgun array (12 L)	Airgun array (12 L)	Single air-gun (0.33 L)	Pure tone (300 Hz)
Max signal BW (Hz)	300-500	300-500	300-500	20-70 100-200	300 (narrow band)
Most sensitive BW** (Hz)	150-900	100-300	100-300	70-400	100-400
Lowest threshold (dB re 1 μPa)	64	87	106	86	106
Received SEL (dB re 1 μPa^2-s)	183	185	187	187^	213
Received SPL (dB re 1 μPa)	205 (peak)	207 (peak)	210 (peak)	209^^ (peak)	180 (peak)
Max Relative motion (nm)	5841	126	289	605	26.7
Excess relative motion (dB)	107	75.4	67.2	82.7	64.8
Reference	Popper et al. (2005)	Popper et al. (2005)	Popper et al. (2005)	McCauley et al. (2003)	Hastings et al. (1996)

* max adult length from Froese, R. and D. Pauly, Editors (2009).FishBase World Wide Web electronic publication, www.fishbase.org, version (04/2009).

** end points defined by minimum threshold + 10 dB

^ personal communication

^^ estimated for 10-m range from 222.6 dB p-p source; cylindrical spreading (depth 9 m)

Some other important items revealed in Table 2 are that the specimens used in the two studies showing hair cell damage are not wild animals and are the most juvenile ones listed (both about 20% of full adult length). McCauley et al. (2005) obtained pink snapper from an aquaculture farm and they were 230±24 mm long on the day of exposure. Length-weight data and auditory thresholds for red seabream (*Pagrus major*) presented by Ishioka et al. (1988) and Iwashita et al. (1999) indicate that McCauley et al.'s pink snapper specimens were about 3 years old.

Several studies, including Iwashita et al (1999) for *P. major*, have shown that hearing is not fully developed in juvenile fish, even up to 3-4 years of age, because of continuing growth of the otoliths and hair cells in the inner ear. In addition aquaculture fish can have different biochemistry and physiology than those reared in the wild and it is not known how this might affect the auditory system (Popper et al. 2007; Mustafa et al. 1995). Popper et al. (2007) found significant TTS in one group of aquaculture rainbow trout (*Oncorhynchus mykiss*) exposed to low frequency active sonar, but not in a second one. They also found large differences in baseline and control thresholds between the two groups. The TTS in the first group had not recovered after 48 hours, when the study ended without further data collection, so the overall results are somewhat confounded due to the differences in the two groups of aquaculture specimens. Given all the issues associated with using aquaculture specimens, including being reared in a noisy environment, random samples of wild adult fish would probably be the best subjects for sound exposure studies. The use of relatively young aquaculture fish likely contributed to the inconsistent results among fish groups in the McCauley et al. (2003) study.

CONCLUSIONS

The results of this study indicate that a lumped parameter dynamic model of the peripheral auditory systems in fishes, which is formulated from fundamental principles, can predict auditory sensitivity and potentially the occurrence of physical damage to fish auditory systems based on calculation of the relative motion between the otoliths and sensory epithelia in the inner ear as a function of frequency. Application of the model to four species in two studies also indicated that excess relative motion in the inner ear was a potentially useful metric to correlate with TTS and hair cell damage. More case studies are needed to validate this finding.

The results also revealed that a major difference between the McCauley et al. (2003) study and the Popper et al. (2005) study was the spectrum levels at low frequencies in the received signals. The Popper et al. spectrum levels contained no energy below 50 Hz and little energy below 200 Hz while the received signals in the McCauley et al. study had maximum energy below 50 Hz and little energy above 1000 Hz. In addition the pink snapper model predicted relatively good auditory sensitivity below 100 Hz, indicating that its ears would be stimulated by the low frequency energy. The absence of low frequencies in Popper et al.'s received signal could have been due to the physical configuration of their source and receiver in a water depth of only 1.9 meters. The Popper et al. (2005) study also used wild specimens caught on site while McCauley et al. used relatively young specimens obtained from an aquaculture facility. Other researchers, including Popper et al. (2007), have reported problems with using juvenile fish or aquaculture fish in sound exposure studies so neither is recommended for use in future studies to examine the effects of sound on fishes. The use of young aquaculture fish is a likely contributor to the discrepancies in results among fish groups found in the McCauley et al. study.

REFERENCES

Danak, A. D. and Hastings, M. C. (2001). Analysis of an ultrasonic biological sensory system. In *Proc. ASME Noise Control and Acoust. Div., NCA-Vol. 28* (R. Marboe *et al*., eds.), The American Society of Mechanical Engineers, New York.

Derenburger, C. (1997). An experimental study of the low-frequency response of the peripheral auditory organs in the goldfish (*Carassius auratus*) and oscar (*Astronotus ocellatus*). M.S. Thesis, Department of Mechanical Engineering, The Ohio State University, Columbus, Ohio.

Enger, P. S. (1981). Frequency discrimination in teleosts—central or peripheral? In Hearing and Sound Communication in Fishes (W. N. Tavolga, A. N. Popper and R. R. Fay, eds.), Springer-Verlag, New York, NY, 243-255.

Finneran, J. J. and Hastings, M. C. (2000). A mathematical analysis of the peripheral auditory system mechanics in the goldfish (Carassius auratus). J. Acoust. Soc. Am. 108, 3035-3043.

Hastings, M. C., Popper, A. N., Finneran, J. J. and Lanford, P. (1996). Effects of low frequency sound on hair cells of the inner ear and lateral line of the teleost fish, *Astronotus ocellatus*. J. Acoust. Soc. Am. 99, 1759-1766.

Hawkins, A. D. And Johnstone, A. D. F. (1978). The hearing of the Atlantic salmon, *Salmo salar*. J. Fish Biol. 13, 655-673.

Ishioka, H., Hatakeyama, Y. and Sakaguchi, S. (1988). The hearing ability of the red sea bream *Pagrus major*. Bull. Jap. Soc. Fisheries Sci. (Nippon Suisan Gakkaishi) 54, 947-951.

Iwashita, A., Sakamoto, M., Kojima, T., Watanabe, Y. And Soeda, H. (1999). Growth effects on the auditory threshold of red sea bream. Bull. Jap. Soc. Fisheries Sci. 65, 833-838.

Kenyon, T. N., Ladich, F. and Yan, H. Y. (1998). A comparative study of hearing ability in fishes: the auditory brainstem response approach. J. Comp. Physiol. A 182, 307-318.

Mann, D. A., Cott, P. A., Hanna, B. W. and Popper, A. N. (2007). Hearing in eight species of northern Canadian freshwater species. J. Fish Biol. 70, 109-120.

McCauley, R. D., Fewtrell, J. and Popper, A. N. 2003. High intensity anthropogenic sound damages fish ears, J. Acoust. Soc. Am. 113, 638-642.

Mustafa, MD. G., Umino, T. and Nakagawa, H. 1995. A comparison of body constituents of wild and cultured red sea bream, *Pagrus major* from different localities in Japan. Asian Fisheries Sci. 8, 143-150.

Popper, A. N., Smith, M. E., Cott, P. A., Hanna, B. W., MacGillivray, A. O., Austin, M. E and Mann, D. A. 2005. Effects of exposure to seismic airgun use on hearing of three fish species, J. Acoust. Soc. Am. 117, 3958-3971.

Popper, A. N., Halvorsen, M. B., Kane, A., Miller, D. L., Smith, M. E., Song, J., Stein, P., and Wysocki, L. E. 2007. The effects of high-intensity, low-frequency active sonar on rainbow trout. J. Acoust. Soc. Am. 122, 623-635.

Song, J., Mann, D. A., Cott, P. A., Hanna, B. W. and Popper, A. N. (2008). The inner ears of Northern Canadian freshwater fishes following exposure to seismic air gun sounds. J. Acoust. Soc. Am. 124, 1360-1366.

Yan, H. Y. and Popper, A. N. (1992). Auditory sensitivity of the cichlid fish *Astronotus ocellatus* (Cuvier). J. Comp. Physiol. A 171, 105-109.

APPENDIX A

MATLAB® Scripts

```
% WOFish.m script
% Model of the peripheral auditory system with Weberian ossicles
% Parameters set for Lake chub (Popper et al. 2005; Mann et al. 2007; Song et
al. 2008)
% Modified 2009 from goldfish.m by MCH

clear
global TRUE FALSE j rhoW cW Pa frequencyArray w s kW

% Define global variables
j = sqrt(-1);
rhoW = 1000;            % density of water (kg/m^3)
cW = 1500;              % sound speed in water (m/s)

% Stimulus information
    startFreq = 10;             % (Hz)
    stopFreq = 5000;            % (Hz)
    pressureAmp = 1.0;          % (Pa)

% Setup frequency and pressure arrays
frequencyArray = ([logspace(log10(startFreq), 3, 75)
linspace(1050,stopFreq,75)])';
Pa= pressureAmp*ones(size(frequencyArray));

w = 2*pi*frequencyArray;                % array of w (rad/s)
s = j*w;                                % Laplace variable
kW = w./cW;                             % acoustic wave number

TRUE = 1;
FALSE = 0;

% Fish parameters
    massFish = 8.6;             % g
    lengthFish = 0.088;         % m

% Geometrical properties of swimbladders
    R1 = 6.138e-3;              % (m)
    R2 = 5.105e-3;              % (m)
    d12 = 0.6e-3 + R1 + R2; % (m)

% Dynamic properties of swimbladder chambers
% k's   (N/m^3)
% b's   (Ns/m^3)
% m's   (kg/m^2)
    k1 = 3.67e6/R1;
    b1 = 500/R1;
    m1 = 5600*R1;
    k2 = 1.68E+06/R2;
    b2 = 420/R2;
    m2 = 9150*R2;
    k12 = 7.62E+07;
    b12 = 12600;

% ****** Tunica externa properties ******************
    hTE = 0.1e-3;
```

```
    Ate = 6.0e-6;
    hL = 0.1e-3;
    visL = 0.1;
    T1overR1 = 0.2;

% ****** Weberian ossicle properties ******************
    KL1 = 7.5e5;        %(N/m)
    KL2 = 450;          %(N/m)

% ****** Weberian canal properties ******************
    rigidCanals = TRUE;
    C3 = 3e-18;                     % (m^3/Pa)
    Df3 = 0.0004*lengthFish;    % (m)

% ****** saccule properties ******************
    ms = 0.3e-6;                    %  (kg)
    Lsg = 0.00157;                  % (m)
    Dsg = 0.29e-3;                  %  (m)
    Ktotal =0.25*1.35e-3;
    Nhc = 147000*lengthFish/4;

% Define coordinates

    rSource_f = [-1000 0 0];

    r1_f = [0 0 0];
    r2_f = [d12*1000 0 0];
    rSac_f = [-13.6 0.75 2.27];
    r1_s = (r1_f - rSource_f)/1000;
    r2_s = (r2_f - rSource_f)/1000;
    rSac_s = (rSac_f - rSource_f)/1000;
    rSac_1 = (rSac_f - r1_f)/1000;
    rSac_2 = (rSac_f - r2_f)/1000;
    clear r1_f r2_f rSac_f rSource_f

% Solve for swimbladder velocities
Zsb1 = m1.*s + b1 + b12 + (k1 + k12)./s;                 % (Ns/m^3)
Zsb2 = m2.*s + b2 + b12 + (k2 + k12)./s;                 % (Ns/m^3)

% **** Coupling coefficients ******************
m12 = rhoW * exp(-j*kW*d12) * R2^2/d12;                  % (kg/m^2)
m21 = rhoW * exp(-j*kW*d12) * R1^2/d12;                  % (kg/m^2)
Z12 = m12.*s + b12 + k12./s;                             % (Ns/m^3)
Z21 = m21.*s + b12 + k12./s;                             % (Ns/m^3)

r1_l = sqrt(r1*r1');
r2_l = sqrt(r2*r2');
G12 = r1_l/r2_l*exp(-j*kW*(r2_l-r1_l));

% **** Solve for V1, V2 ********************
V1 = -(Zsb2-G12.*Z12)./(Zsb1.*Zsb2-Z12.*Z21);               % (m/s)
V2 = -(G12.*Zsb1-Z21)./(Zsb1.*Zsb2-Z12.*Z21);               % (m/s)
```

```
% Setup equations and solve for Web. App. velocities and pressures
    Get tunica externa impedances Zte, ZL and consatnt Gt (tunicaExterna.m)
    Mte = tunicaExterna(R1, Ate, hTE, hL, visL, T1overR1);
    Zte = Mte(:,1); ZL = Mte(2,2); Gt = Mte(1,2);
    clear Mte;

% Get dynamic parameters for Weberian ossicles  (webOssicles.m)
    Mossicles = webOssicles(Zte, ZL, KL1, KL2, lengthFish);
    Ztr = Mossicles(:,1); Z3 = Mossicles(:,2); Zic = Mossicles(:,3);
    Z4= Mossicles(:,4); Zsc = Mossicles(:,5);
    GL = Mossicles(1,6); Acl = Mossicles(2,6);
    clear Mossicles;

% Get dynamic parameters for Weberian apparatus fluid canals  (webCanals.m)
    Mcanals = webCanals(lengthFish, C3, Df3);
    Zfc = Mcanals(:,1); Atc = Mcanals(2,8);
    Zfc1 = Mcanals(:,2); Zfc2 = Mcanals(:,3); Zfc3 = Mcanals(:,4);
    Zc1 = Mcanals(:,5); Zc2 = Mcanals(:,6); Zc3 = Mcanals(:,7);
    clear Mcanals;

    % rigid-walled canal solution
    D = (Z3.^2).*(Zsc+Acl^2*Zfc)-Zic.*Ztr.*Zsc-
Acl^2*Zic.*Ztr.*Zfc+(Z4.^2).*Ztr;
    Vsc = -(GL*Gt*Z3.*Zte.*Z4)./D.*V1;
    Vic = -(GL*Gt*Z3.*Zte).*(Zsc+Acl^2*Zfc)./D.*V1;
    V3 = GL*Gt*Zte.*V1.*(-Zic.*Zsc-Acl^2*Zic.*Zfc+Z4.^2)./D;
    Psi = -Acl*GL*Gt*Z3.*Zte.*V1.*Z4.*Zfc./D;
    Vsa = Acl/Atc.*Vsc;


Vt = GL*V3;

clear x A b Zsb1 Zsb2 Z12 Z21 Zte Ztr Zic Z3 Z4 Zsc Zfc
clear n ZL S1 S2 Acl Atc GL Gt D


% Get indirect path particle velocity vector at the saccule
    RP1 = sqrt(rp1*rp1');          %   ||rp1||
    RP2 = sqrt(rp2*rp2');          %   ||rp2||

    t1 = (1+j*kW*RP1);
    t2 = (R1/RP1)^2;
    t3 = exp(-j.*kW.*(RP1-R1));
    va1 = t1*t2.*V1.*t3;

    t1 = (1+j*kW*RP2);
    t2 = (R2/RP2)^2;
    t3 = exp(-j.*kW.*(RP2-R2));
    va2 = t1*t2.*V2.*t3;

    for n = 1 : length(w),
        Va1(n,1:3) = va1(n)*rp1/RP1;
        Va2(n,1:3) = va2(n)*rp2/RP2;
    end
```

```
    Va = Va1 + Va2;
% Get direct path particle velocity vector at the saccule
    Constants = zeros(size(s));

    RP = sqrt(rp*rp');          %   ||rp||
    R1 = sqrt(r1*r1');          %   ||r1||
    va = (1-j./kW/RP)*R1/RP.*Pa./rhoW/cW.*exp(-j.*kW.*(RP-R1));

    for n = 1 : length(w),
        Va(n,1:3) = va(n)*rp/RP;
    end

% Solve for sagitta motion, HC shear using 1-D sagitta model
    Msaccule = saccule1D(lengthFish, massFish, ms, Lsg, Dsg, Ktotal, Nhc, Vd,
Vi, Vsa);
    vDirect = Msaccule(:,1); vIndirect = Msaccule(:,2);
    vWeb = Msaccule(:,3); Xrel = Msaccule(:,4);
    Xsg = Msaccule(:,5); Xse = Msaccule(:,6);
    Hse = Msaccule(:,7); Hsa = Msaccule(:,8);
    clear Msaccule

% Define relative motions / phases
rp=r1_s;
r1=r1_s;

Constants = zeros(size(s));

    RP = sqrt(rp*rp');          %   ||rp||
    R1 = sqrt(r1*r1');          %   ||r1||
    va = (1-j./kW/RP)*R1/RP.*Pa./rhoW/cW.*exp(-j.*kW.*(RP-R1));

    for n = 1 : length(w),
        Va(n,1:3) = va(n)*rp/RP;
    end

Vay = Va(:,2);          % velocity is v(y)

Ed = 0.5*densityWater*(abs(Vay).^2+(abs(Pa)./densityWater./speedWater).^2);

f = frequencyArray;

RM1 = abs(V1)./sqrt(Ed / densityWater)./densityWater./speedWater./1e-6;
RM2 = abs(V2)./sqrt(Ed / densityWater)./densityWater./speedWater./1e-6;
RM3 = abs(V3)./sqrt(Ed / densityWater)./densityWater./speedWater./1e-6;
RMT = abs(Vt)./sqrt(Ed / densityWater)./densityWater./speedWater./1e-6;
RMic = abs(Vic)./sqrt(Ed / densityWater)./densityWater./speedWater./1e-6;
RMsc = abs(Vsc)./sqrt(Ed / densityWater)./densityWater./speedWater./1e-6;
RMsa = abs(Vsa)./sqrt(Ed / densityWater)./densityWater./speedWater./1e-6;
phase1 = 180/pi*unwrap(angle(V1));
phase2 = 180/pi*unwrap(angle(V2));
phase3 = 180/pi*unwrap(angle(V3));
phaseT = 180/pi*unwrap(angle(Vt));
phaseIC = 180/pi*unwrap(angle(Vic));
```

```
phaseSC = 180/pi*unwrap(angle(Vsc));
phaseSA = 180/pi*unwrap(angle(Vsa));

Ddirect = abs(vDirect./s)./sqrt(Ed /
densityWater)./densityWater./speedWater./1e-9;
Dindirect = abs(vIndirect./s)./sqrt(Ed /
densityWater)./densityWater./speedWater./1e-9;
Dweb = abs(vWeb./s)./sqrt(Ed / densityWater)./densityWater./speedWater./1e-9;
phaseDirect = 180/pi*unwrap(angle(vDirect./s));
phaseIndirect = 180/pi*unwrap(angle(vIndirect./s));
phaseWeb = 180/pi*unwrap(angle(vWeb./s));

Dsg = abs(Xsg)./sqrt(Ed / densityWater)./densityWater./speedWater./1e-9;
Dse = abs(Xse)./sqrt(Ed / densityWater)./densityWater./speedWater./1e-9;
Drel = abs(Xrel)./sqrt(Ed / densityWater)./densityWater./speedWater./1e-9;
phaseSE = 180/pi*(angle(Xse));
phaseSG = 180/pi*unwrap(angle(Xsg));
phaseSE = 180/pi*unwrap(angle(Xse));
phaseRel = 180/pi*unwrap(angle(Xrel));

hstart = 50;
vstart = 50;
hsize = 450;
vsize = 525;
pos = [hstart vstart hsize vsize];
currentFig = 1;
lineWidth = [1.0 0.5 1.0 2.0 0.5 0.5];
borderWidth = 1.0;
fontSize = 10;
legendWidth = 0.75;

figure(currentFig);
subplot(2,1,1);
    lineH = loglog(f,Drel, 'r-');
    for hn = 1 : length(lineH)
        set(lineH(hn),'LineWidth',[lineWidth(hn)]);
    end
    set(gca,'LineWidth',[borderWidth]);
    set(gca,'FontSize',[fontSize]);
    set(gca,'XTickLabel',[10 100 1000 10000]);
    xlabel('frequency (Hz)')
    ylabel('amplitude (nm/Pa)')
%   legendH = legend(' rel ',-1);
%   set(legendH,'LineWidth',[legendWidth]);
    title(['normalized relative displacement'])
subplot(2,1,2);
    lineH = semilogx(f,phaseRel, 'r-');
    for hn = 1 : length(lineH)
        set(lineH(hn),'LineWidth',[lineWidth(hn)]);
    end
    set(gca,'LineWidth',[borderWidth]);
    set(gca,'FontSize',[fontSize]);
    set(gca,'YLim',[-360 360],'YTick',[-360 -180 0 180 360]);
    set(gca,'XTickLabel',[10 100 1000 10000]);
    xlabel('frequency (Hz)')
    ylabel('phase (deg)')
```

```
%   legendH = legend(' rel ',-1);
%   set(legendH,'LineWidth',[legendWidth])

function QoutTE = tunicaExterna(R1, teComplianceConstant, teThickness, 
gapThickness, gapViscosity, slitRatio)

    eval('global j TRUE FALSE rhoW cW Pa frequencyArray w s kW');
    Constants = zeros(size(s));

% ****** Tunica externa properties ******************
    teRadius = R1;                            % (m)
    slitRadius = slitRatio * teRadius;        % (m)

% Use power function
    teCompliancePower = 0.26;
    teCompliance = teComplianceConstant * gamma(teCompliancePower + 
1)./s.^(teCompliancePower); % (m^2/N)

% ****** TE dynamic parameters ********************
    ZL = 2. * pi *teRadius^2 * gapViscosity / gapThickness;     % (Ns/m)
    Zte = 4. * pi * teRadius * teThickness * slitRadius / (4. * teRadius^2 - 
slitRadius^2) ./ (s.*teCompliance);    % (Ns/m)
    Gt = 4. * teRadius / slitRadius;

% ****** Define variables to output ******************

    Constants(2,1) = ZL;
    QoutTE = [Zte Constants];
```

```
 function Qoutweb = web(Zte, ZL, KL1, KL2, lengthFish);

eval('global j TRUE FALSE rhoW cW Pa frequencyArray w s kW');
Constants = zeros(size(s));

% density of fish bone
densityFishBone = 1805;                    % kg/m^3

% ********* Tripus ****************

rhoT = densityFishBone;                            % kg/m^3
LT = 0.060*lengthFish;                             % m  (overall length)
a1 = 0.39*LT;           b1 = 0.43*LT;       % m  (The following are
a2 = 0.27*LT;               b2 = 0.37*LT;       % m   estimated from
b3 = 0.68*LT;               a4 = 0.21*LT;       % m   Cyprinus carpio
b4 = 0.36*LT;               b5 = 0.15*LT;       % m   and exp's on goldfish)
d4 = 0.19*LT;                                        % m
tT = 0.07*LT;                                        % m  (thickness of
tripus)

Jt = 1.5*rhoT*tT*(a1*b1/3*(a1^2+b1^2)-
a2*b2/12*(a2^2+b2^2+6*b1^2)+pi*a1*b3/16*(a1^2+b3^2)-
pi*a4*b4/16*(a4^2+b4^2+4*d4^2)-a4*b5/12*(a4^2+b5^2+6*d4^2));

% Define lengths of effective lever arms for mechanical connections
l1 = 0.20 * LT;     % m  Ligament L1
l2 = 0.15 * LT;     % m  Ligament L2
l3 = 0.38 * LT;     % m  Ligament L3
lTE = 0.62 * LT; % m  Insertion of Tunica Externa
G1 = l1 / l3;
G2 = l2 / l3;
GL = lTE / l3;

% ********* Intercalarium ****************

rhoI = densityFishBone;                    % kg/m^3
LI = 0.20*LT;                                      % m
R1 = 0.025*LT;     L1 = 0.19*LT;    % m
R2 = 0.01*LT;       L2 = 0.06*LT;    % m
R3 = 0.01*LT;       L3 = 0.08*LT;    % m
theta2 = pi/180*(-75);                 % rad
theta3 = pi/180*32.5;                      % rad
li = 0.20 * LT;                                % m
% Distances for transfer of axes
di1 = abs(L1/2-L2*(cos(theta2)+j*sin(theta2)));
%m
di2 = L2/2;
%m
di3 = abs(L3/2*(cos(theta3)+j*sin(theta3))-L2*(cos(theta2)+j*sin(theta2)));
%m

Ji =
1.5*rhoI*pi*((R1^4*L1+R2^4*L2+R3^4*L3)/4+(R1^2*L1^3+R2^2*L2^3+R3^2*L3^3)/12
+(R1^2*L1*di1^2+R2^2*L2*di2^2+R3^2*L3*di3^2));
```

```
% *************** Scaphium ************************

rhoS = densityFishBone;    % (kg/m^3)
ls = 0.11 * LT;      % (m)
a = 0.11 * LT;       % (m)
b = 0.11 * LT;           % (m)
c = 0.04 * LT;           % (m)
Acl = pi*a*b;

Js = 1.5*4/30*rhoS*pi*(a*b*c*(6*b^2+c^2));          %kgm^2

% Tripus/intercalarium ligaments

Z1 = KL1./s;                                %Nsec/m
Z2 = KL2./s;                                %Nsec/m
KL3 = KL1;                       Z3 = KL3./s + 0.01*Zte;         %Nsec/m
KL4 = KL1;                       Z4 = KL4./s + 0.01*Zte;         %Nsec/m


Zt = Jt/(l3)^2*s+G1^2*Z1+G2^2*Z2+GL^2*Zte+GL^2*ZL+Z3;   %Nsec/m
Zi = Ji/(li)^2*s+Z3+Z4;
%Nsec/m
Zs = Js/(ls)^2*s+Z4;
%Nsec/m

Constants(1) = GL;
Constants(2) = Acl;
Qoutweb = [Zt Z3 Zi Z4 Zs Constants];

return
```

```
function Qoutcanals = webCanals(lengthFish, C3, Df3);

eval('global j TRUE FALSE rhoW cW Pa frequencyArray w s kW');
Constants = zeros(size(s));

% Section 1
    rho(1) = 1008;
    D(1) = 0.022*lengthFish;    % m
    L(1) = 0.029*lengthFish;    % m
    A(1) = pi*D(1)^2/4;     % m^2
    u(1) = 0.76e-3;         %Ns/m^2
% Section 2
    rho(2) = 1010;
    D(2) = 0.01*lengthFish;     % m
    L(2) = 0.059*lengthFish;    % m
    A(2) = pi*D(2)^2/4;     % m^2
    u(2) = 1.20e-3;         %Ns/m^2
% Section 3
    rho(3) = 1010;
    D(3) = Df3;
    L(3) = 0.007*lengthFish;    % m
    A(3) = pi*D(3)^2/4;     % m^2
    u(3) = 1.20e-3;         %Ns/m^2


for m = 1:3
    w0 = u(m)/rho(m)/D(m)^2;
    M1 = 4./3.*rho(m)/A(m)*L(m);
    M2 = rho(m)/A(m)*L(m);
    R1 = 128*u(m)*L(m)/pi/D(m)^4;
    R2 = 8*L(m)/pi/D(m)^3*sqrt(2*rho(m)*u(m)*w);
    R20 = 8*L(m)/pi/D(m)^3*sqrt(2*rho(m)*u(m)*7200*w0);

    for n = 1: length(w)
        if (w(n) < 32*w0)
            M(n,m) = M1;
            R(n,m) = R1;
        elseif (w(n) > 7200*w0)
            M(n,m) = M2;
            R(n,m) = R2(n);
        else
            M(n,m) = M1 + (M2-M1)/(7200*w0-32*w0)*(w(n)-32*w0);
            R(n,m) = R1 + (R20-R1)/(7200*w0-32*w0)*(w(n)-32*w0);
        end
    end
end


% Mechanical impedances (P/Q) of each section
Zfc1 = M(:,1).*s + R(:,1);
Zfc2 = M(:,2).*s + R(:,2);
Zfc3 = M(:,3).*s + R(:,3) + (1.)./C3./s;

Zfc = (2 * Zfc1 + 2 * Zfc2 + Zfc3);
```

```
% Total estimated fluid compliance (m^3/Pa)
Bl = 2.18e9;    % bulk modulus of water N/m2
E = 1e9;            % modulus for collagen  N/m2
c1 = (10/E+1/Bl)*A(1)*L(1);
c2 = (10/E+1/Bl)*A(2)*L(2);
c3 = (10/E+1/Bl)*A(3)*L(3);
Zc1 = (1.)./j./w/c1;
Zc2 = (1.)./j./w/c2;
Zc3 = (1.)./j./w/c3;

Constants(1, 1) = A(1);
Constants(2, 1) = A(3);
Qoutcanals = [Zfc Zfc1 Zfc2 Zfc3 Zc1 Zc2 Zc3 Constants];

return
```

```
function QoutSaccule1D = saccule1D(lengthFish, massFish, ms, Lsg, Dsg,
Ktotal, Nhc, Vd, Vi, Vsa)

eval('global j TRUE FALSE rhoW cW Pa frequencyArray w s kW');
Constants = zeros(size(s));


    Q = pi/6;
    R = [-cos(Q) 0 sin(Q);0 -1 0;sin(Q) 0 cos(Q)];

    for n =1:length(w),
        VdSac(1:3,n) = R*Vd(n,1:3)';
        ViSac (1:3,n) = R*Vi(n,1:3)';
    end

    %   Endolymph properties
    rhoE = 1010;                % kg/m^3
    visE = 10.0e-3;         % Ns/m^2

    %   Saccular otolith properties
    rhoS = 2930;                            % kg/m^3
    Vol = ms/rhoS;                      % m^3
    Vadd = 1*Vol;                           % m^3
    me = rhoE*Vadd + ms;            % effective mass


    Kgs = 0.225*Ktotal;     % N/m
    Ksp = 0.375*Ktotal;     % N/m
    Ksof = 0.400*Ktotal;        % N/m
    Bsof = 0.027e-6;            % Ns/m
    Bcb = 6e-6;                 % Ns/m
    Zhc = Kgs*Bcb./(Bcb*s+Kgs)+Ksp./s+Ksof./s+Bsof;


    w0 = w./(2*visE/rhoE/(Dsg/2)^2);
    Zcyl = 2*pi*Lsg*visE*(1 + 2*sqrt(w0)+j*sqrt(w0).*(2+sqrt(w0)));


    Zom = Inf * ones(size(w));
    Zsg = me*(1+Zhc./Zom).*s+Nhc*Zhc+Zcyl.*(1+Zhc./Zom);

    Zm = ms*(1-rhoE/rhoS).*s;
    Zf = rhoE*(Vol+Vadd)*s + Zcyl;

    vDirect =   -Zm./Zsg.*VdSac(3,:)';
    vIndirect =     -Zm./Zsg.*ViSac(3,:)';
    vWeb =      -Zf./Zsg.*Vsa;

    Xse = (VdSac(3,:)'+ViSac(3,:)')./s;
    Xsa = Vsa./s;

    Hse = -Zm./Zsg;
```

```
    Hsa = -Zf./Zsg;
    Xrel = Hse.*Xse + Hsa.*Xsa;

    Zm2 = rhoE*(Vol+Vadd)*s + Zcyl+ Nhc*Zhc;
    Xsg = Zm2./Zsg.*Xse - Zf./Zsg.*Xsa;

    QoutSaccule1D = [vDirect vIndirect vWeb Xrel Xsg Xse Hse Hsa];

return
```

```
% GenFish.m script
% Model of the peripheral auditory system without Weberian ossicles
% Modified 2009 from goldfish.m by MCH

Clear
global TRUE FALSE j rhoW cW Pa frequencyArray w s kW

% Define global variables
j = sqrt(-1);
rhoW = 1000;            % (kg/m^3)
cW = 1500;              %  (m/s)

% Stimulus information
    startFreq = 10;             % (Hz)    stopFreq = 5000;            % (Hz)
    pressureAmp = 1.0;          % (Pa)

% Setup frequency and pressure arrays
frequencyArray = ([logspace(log10(startFreq), 3, 75)
linspace(1050,stopFreq,75)])';
Pa= pressureAmp*ones(size(frequencyArray));

w = 2*pi*frequencyArray;                % array of w (rad/s)
s = j*w;                                % Laplace variable
kW = w./cW;                             % acoustic wave number
TRUE = 1;
FALSE = 0;
% Fish parameters
    massFish = 26.4;            % g
    lengthFish = 0.083;         % m
    R1 = 5.99e-3;               % (m)
% Dynamic properties of swimbladder chambers
% k's   (N/m^3)
% b's   (Ns/m^3)
% m's   (kg/m^2)
    k1 = 3.67e6/R1;
    b1 = 500/R1;
    m1 = 2500*R1;

% ****** saccule properties ******************
    ms = 2.46e-7;                   % (kg)scaled with GF mass
    Lsg = 0.00278;                  % sagitta length (m)
    Dsg = 1.11e-3;                  % sagitta diameter (m)
    Ktotal = 0.8*1.35e-3;           % (N/m)GF baseline
    Nhc = 0.65*147000*lengthFish;      % GF baseline (scaled length)

% Define coordinates
    rSource_f = [-1000 0 0];
    if rSource_f(1) < 0
        location = ['source in front (' num2str(abs(rSource_f(1)/1000)) '
m)'];
    else
        location = ['source behind (' num2str(abs(rSource_f(1)/1000)) ' m)'];
    end

%   Define organ locations in fish coordinates
```

```
    r1_f = [0 0 0];
%   r2_f = [d12*1000 0 0];
    rSac_f = [-16.7 0.71 2.1];
    r1_s = (r1_f - rSource_f)/1000;
%   r2_s = (r2_f - rSource_f)/1000;
    rSac_s = (rSac_f - rSource_f)/1000;
    rSac_1 = (rSac_f - r1_f)/1000;
%   rSac_2 = (rSac_f - r2_f)/1000;
%   clear r1_f r2_f rSac_f rSource_f
    clear r1_f rSac_f rSource_f

  % Solve for swimbladder velocity
Zsb1 = m1.*s + b1 + (k1)./s;            % (Ns/m^3)
V1 = -Pa./(Zsb1);                       % (m/s)

% Get indirect path particle velocity vector at the saccule
rp1 = rSac_1;
RP1 = sqrt(rp1*rp1');

    t1 = (1+j*kW*RP1);
    t2 = (R1/RP1)^2;
    t3 = exp(-j.*kW.*(RP1-R1));
    va1 = t1*t2.*V1.*t3;

    for n = 1 : length(w),
        Va1(n,1:3) = va1(n)*rp1/RP1;
    end

    Vi = Va1;

% Get direct path particle velocity vector at the saccule
    Vd = getDirectField(rSac_s, r1_s);

    Vsa = zeros(size(frequencyArray));

% Solve for sagitta motion, HC shear using 1-D sagitta model
    Msaccule = saccule1D(lengthFish, massFish, ms, Lsg, Dsg, Ktotal, Nhc, Vd,
Vi, Vsa);
    vDirect = Msaccule(:,1); vIndirect = Msaccule(:,2);
    vWeb = Msaccule(:,3); Xrel = Msaccule(:,4);
    Xsg = Msaccule(:,5); Xse = Msaccule(:,6);
    Hse = Msaccule(:,7); Hsa = Msaccule(:,8);
    clear Msaccule

% Define relative motions / phases
speedWater = cW;
densityWater = rhoW;
% Get acoustic parameters at SB due to direct field (getDirectField.m)
Mdirect = getDirectField(r1_s, r1_s);
Va = Mdirect(:,2);          % velocity is v(y)
% calculate energy density using velocity y-component only
Ed = 0.5*densityWater*(abs(Va).^2+(abs(Pa)./densityWater./speedWater).^2);

f = frequencyArray;
```

```
Ddirect = abs(vDirect./s)./sqrt(Ed /
densityWater)./densityWater./speedWater./1e-9;
Dindirect = abs(vIndirect./s)./sqrt(Ed /
densityWater)./densityWater./speedWater./1e-9;
phaseDirect = 180/pi*unwrap(angle(vDirect./s));
phaseIndirect = 180/pi*unwrap(angle(vIndirect./s));

Dsg = abs(Xsg)./sqrt(Ed / densityWater)./densityWater./speedWater./1e-9;
Dse = abs(Xse)./sqrt(Ed / densityWater)./densityWater./speedWater./1e-9;
Drel = abs(Xrel)./sqrt(Ed / densityWater)./densityWater./speedWater./1e-9;
%phaseSG = 180/pi*(angle(Xsg));
%phaseSE = 180/pi*(angle(Xse));
%phaseRel = 180/pi*(angle(Xrel));
phaseSG = 180/pi*unwrap(angle(Xsg));
phaseSE = 180/pi*unwrap(angle(Xse));
phaseRel = 180/pi*unwrap(angle(Xrel));

hstart = 50;
vstart = 50;
hsize = 450;
vsize = 525;
pos = [hstart vstart hsize vsize];
currentFig = 1;
lineWidth = [1.0 0.5 1.0 2.0 0.5 0.5];
borderWidth = 1.0;
fontSize = 10;
legendWidth = 0.75;

figure(currentFig);
subplot(2,1,1);
    lineH = loglog(f,Drel, 'r-');
    for hn = 1 : length(lineH)
        set(lineH(hn),'LineWidth',[lineWidth(hn)]);
    end
    set(gca,'LineWidth',[borderWidth]);
    set(gca,'FontSize',[fontSize]);
    set(gca,'XTickLabel',[10 100 1000 10000]);
    xlabel('frequency (Hz)')
    ylabel('amplitude (nm/Pa)')
%   legendH = legend(' rel ',-1);
%   set(legendH,'LineWidth',[legendWidth]);
    title(['normalized relative displacement'])
subplot(2,1,2);
    lineH = semilogx(f,phaseRel, 'r-');
    for hn = 1 : length(lineH)
        set(lineH(hn),'LineWidth',[lineWidth(hn)]);
    end
    set(gca,'LineWidth',[borderWidth]);
    set(gca,'FontSize',[fontSize]);
    set(gca,'YLim',[-360 360],'YTick',[-360 -180 0 180 360]);
    set(gca,'XTickLabel',[10 100 1000 10000]);
    xlabel('frequency (Hz)')
    ylabel('phase (deg)')
%   legendH = legend(' rel ',-1);
%   set(legendH,'LineWidth',[legendWidth]);
```

```
function [Va] = getDirectField(rp, r1)

    eval('global j TRUE FALSE rhoW cW Pa frequencyArray w s kW');
    Constants = zeros(size(s));

    RP = sqrt(rp*rp');          %   ||rp||
    R1 = sqrt(r1*r1');          %   ||r1||
    va = (1-j./kW/RP)*R1/RP.*Pa./rhoW/cW.*exp(-j.*kW.*(RP-R1));

    for n = 1 : length(w),
        Va(n,1:3) = va(n)*rp/RP;
    end

return
```

```
function QoutSaccule1D = saccule1D(lengthFish, massFish, ms, Lsg, Dsg,
Ktotal, Nhc, Vd, Vi, Vsa)

eval('global j TRUE FALSE rhoW cW Pa frequencyArray w s kW');
Constants = zeros(size(s));


    % Setup rotation matrix to convert velocities to saccule coordinates
    Q = pi/6;
    R = [-cos(Q) 0 sin(Q);0 -1 0;sin(Q) 0 cos(Q)];

    % Find direct and indirect particle velocity in hair cell direction
    for n =1:length(w),
        VdSac(1:3,n) = R*Vd(n,1:3)';
        ViSac (1:3,n) = R*Vi(n,1:3)';
    end

    %   Endolymph properties
    rhoE = 1010;            % kg/m^3
    visE = 10.0e-3;         % Ns/m^2

    %   Saccular otolith properties
    rhoS = 2930;                    % kg/m^3
    Vol = ms/rhoS;                  % m^3
    Vadd = 1*Vol;                   % m^3 (additional volume due to fluid)
    me = rhoE*Vadd + ms;            % effective mass

    %   Single hair cell ciliary bundle properties
    Kgs = 0.225*Ktotal;     % N/m
    Ksp = 0.375*Ktotal;     % N/m
    Ksof = 0.400*Ktotal;        % N/m
    Bsof = 0.027e-6;            % Ns/m
    Bcb = 6e-6;                 % Ns/m
    Zhc = Kgs*Bcb./(Bcb*s+Kgs)+Ksp./s+Ksof./s+Bsof;

    %   Mech impedance for viscous drag on otolith
    w0 = w./(2*visE/rhoE/(Dsg/2)^2);
    Zcyl = 2*pi*Lsg*visE*(1 + 2*sqrt(w0)+j*sqrt(w0).*(2+sqrt(w0)));

    %   Otolithic membrane properties and
    %   sagitta mechanical impedance

    Zom = Inf * ones(size(w));
    Zsg = me*(1+Zhc./Zom).*s+Nhc*Zhc+Zcyl.*(1+Zhc./Zom);

    % Mech impedance of input terms
    Zm = ms*(1-rhoE/rhoS).*s;
    Zf = rhoE*(Vol+Vadd)*s + Zcyl;

    % relative motion due to three pathways
    vDirect =   -Zm./Zsg.*VdSac(3,:)';
    vIndirect =     -Zm./Zsg.*ViSac(3,:)';
    vWeb =      -Zf./Zsg.*Vsa;
```

```
    Xse = (VdSac(3,:)'+ViSac(3,:)')./s;
    Xsa = Vsa./s;

    Hse = -Zm./Zsg;
    Hsa = -Zf./Zsg;
    Xrel = Hse.*Xse + Hsa.*Xsa;

    Zm2 = rhoE*(Vol+Vadd)*s + Zcyl+ Nhc*Zhc;
    Xsg = Zm2./Zsg.*Xse - Zf./Zsg.*Xsa;

    QoutSaccule1D = [vDirect vIndirect vWeb Xrel Xsg Xse Hse Hsa];

return
```

APPENDIX B

Frequency Bands from Spectrum Levels

for

Signals in Popper et al. (2005) and McCauley et al. (2003)

Band Analysis for Figure 2(A) in Popper et al. (2005)

f1 (Hz)	f2(Hz)	Avg SPL	SPL Band	Acoustic Pressure (Pa)
50	100	121.8	138.8	8.7
100	200	121.8	141.8	12.3
200	300	137.7	157.7	76.7
300	400	156.8	176.8	691.8
400	500	150.5	170.5	335.0
500	600	145.5	165.5	188.4
600	700	134.1	154.1	50.7
700	800	149.1	169.1	285.1
800	900	144.9	164.9	175.8
900	1000	150.5	170.5	335.0
1000	1100	143.6	163.6	151.4
1100	1200	129.1	149.1	28.5
1200	1300	141.8	161.8	123.0
1300	1400	148.2	168.2	257.0
1400	1500	143.6	163.6	151.4
1500	1600	143.6	163.6	151.4
1600	1700	141.8	161.8	123.0
1700	1800	141.8	161.8	123.0
1800	1900	141.8	161.8	123.0
1900	2000	141.8	161.8	123.0
2000	2100	137.1	157.1	71.6
2100	2200	143.6	163.6	151.4
2200	2300	143.6	163.6	151.4
2300	2400	137.1	157.1	71.6
2400	2500	143.6	163.6	151.4
2500	2600	137.3	157.3	73.3
2600	2700	137.3	157.3	73.3
2700	2800	137.3	157.3	73.3
2800	2900	140.0	160.0	100.0
2900	3000	140.0	160.0	100.0
3000	3100	140.0	160.0	100.0
3100	3200	124.1	144.1	16.0
3200	3300	125.0	145.0	17.8
3300	3400	130.5	150.5	33.5
3400	3500	127.3	147.3	23.2
3500	3600	130.5	150.5	33.5
3600	3700	130.5	150.5	33.5
3700	3800	128.6	148.6	26.9
3800	3900	128.6	148.6	26.9
3900	4000	130.5	150.5	33.5
4000	4100	135.0	155.0	56.2
4100	4200	137.3	157.3	73.3
4200	4300	132.7	152.7	43.2
4300	4400	135.0	155.0	56.2
4400	4500	132.7	152.7	43.2
4500	4600	130.5	150.5	33.5
4600	4700	130.5	150.5	33.5
4700	4800	128.6	148.6	26.9
4800	4900	134.1	154.1	50.7
4900	5000	132.7	152.7	43.2

Band Analysis for 50-m curve, Figure 2 in McCauley et al. (2003)

f1 (Hz)	f2(Hz)	Avg SPL	SPL Band	Acoustic Pressure (Pa)
10	20	145.5	155.5	59.6
20	30	163.5	173.5	473.2
30	40	143.0	153.0	44.7
40	50	165.9	175.9	623.7
50	60	148.4	158.4	83.2
60	70	161.9	171.9	393.6
70	80	148.4	158.4	83.2
80	90	148.4	158.4	83.2
90	100	148.4	158.4	83.2
100	200	152.4	172.4	416.9
200	300	143.0	163.0	141.3
300	400	140.7	160.7	108.4
400	500	141.8	161.8	123.0
500	600	135.7	155.7	61.0
600	700	132.7	152.7	43.2
700	800	135.7	155.7	61.0
800	900	132.7	152.7	43.2
900	1000	122.7	142.7	13.6
1000	2000	120.3	150.3	32.7